Journal of Alloys and Compounds 588 (2014) 177–181

Contents lists available at ScienceDirect

Journal of Alloys and Compounds

journal homepage: www.elsevier.com/locate/jalcom

Pyroelectric, piezoelectric, elastic and dielectric properties of triglycine – zinc chloride crystal

Z. Tylczyński *, M. Wiesner

Faculty of Physics, Adam Mickiewicz University, Umultowska 85, 61-614 Poznań, Poland

ARTICLE INFO

Article history:
Received 2 October 2013
Received in revised form 31 October 2013
Accepted 1 November 2013
Available online 11 November 2013

Keywords:
Pyroelectric constant
Piezoelectricity
Elastic susceptibility
Dielectric permittivity
Phase transition

ABSTRACT

Temperature changes in the components of pyroelectric, piezoelectric, elastic and dielectric tensors were studied in triglycine zinc chloride crystal in the range 100–300 K. No anomalies in pyroelectric and elastic properties were found. The directions of maximal and minimal values of the elastic susceptibility correspond to the longest and shortest bonds between the Glycine(A)–$ZnCl_2$–Glycine(B) complexes. The attenuations of the resonant vibration along [100], [010] and [001] axes and the corresponding to them d_{31}, d_{32} and d_{33} components have maxima at 220 K. The real part of dielectric permittivity ε_3' shows a big jump at 234 K. The imaginary part of all dielectric components have small dispersion above this temperature. Possible phase transition in triglycine zinc chloride crystal has been discussed.

1. Introduction

The development of highly efficient nonlinear optical materials for optoelectronic and nonlinear optics applications has been the subject of intense research activity over the past two decades. The synthesis of novel and efficient frequency conversion materials has resulted in the development of semi-organic materials in which the organic ligands are ionically bonded with inorganic hosts. The new semi-organic crystals with amino acids show highly efficient optical second harmonic generation and are promising candidates for photonic applications.

Triglycine zinc chloride crystal (named Gly_3–$ZnCl_2$) was first synthesised in 1927 by Dubsky [1] and can be grown to large single crystals of optical quality. Gly_3–$ZnCl_2$ has orthorhombic polar symmetry with the space group $Pbn2_1$. The crystal structure consists of isolated distorted tetrahedral $[Zn(Gly)_2Cl_2]$ clusters connected by hydrogen bonds [2,3]. The linear and nonlinear (the both phase matching conditions are possible) optical properties reported by Fleck et al. [4] and good transmission in the visible and near ultraviolet parts of the spectrum show that Gly_3–$ZnCl_2$ is a promising material for electro- and acousto-optic applications. The other basic physical properties of this crystal are poorly known. The only real part of dielectric permittivity were established in the temperature range above RT and no direction of the measuring field was given [5]. The components piezoelectric tensor were determined by measurement of the electric charge generated by dynamic mechanical low-frequency stress at room temperature [4]. Untill now no data on the pyroelectric coefficient and components of the elasticity tensor and their temperature changes has been published. To the best of our knowledge, there is no information on any possible phase transition in temperatures below RT.

Studies of complex permittivity, pyroelectric and piezoelectric coefficients and elastic susceptibility, in the temperature range from RT to 100 K are presented in the paper.

2. Experimental procedures

To grown Gly_3–$ZnCl_2$ crystals from the nuclei, the glycine and zinc chloride were dissolved in deionised water at stoichiometric ratio. Defect-free monocrystals were obtained at a temperature of 305 K using the rotation seed method. Good quality crystals of the size up to a few cm^3 were obtained after 1–1.5 month. The monocrystals typically show big orthorhombic pyramids. With reference to the well-developed morphological faces the orientation of samples was adjusted.

Crystal of Gly_3–$ZnCl_2$ has orthorhombic symmetry with the point group mm2. Nonzero components of piezoelectric tensor: d_{31}, d_{32}, d_{33}, d_{24} and d_{15} were determined for the samples cut out from large monocrystals – its orientations are presented in Fig. 1.

Piezoelectric properties studied by the series resonance method were performed using a computer controlled Agilent 4294A impedance meter with a frequency step of 10 Hz. The measuring field was 1 V $mm^{-1}$and its frequency ranged from 50 kHz up to 5 MHz. For the electric field applied along the direction [001], the components of the tensors of electro-mechanical coupling, elastic susceptibility and piezoelectricity were calculated from the following relations [6]:

- for transversal piezoelectric phenomenon for normal vibration along the length of plates:

$$(k_{3j}^2)' = 1 - \left\{\frac{\pi}{2}\frac{f_r}{f_a}\tan\left(\frac{\pi}{2}\frac{f_a - f_r}{f_r}\right)\right\}^{-1}, \quad (1)$$

---

* Corresponding author.
E-mail address: zbigtyl@amu.edu.pl (Z. Tylczyński).

0925-8388/$ - see front matter
http://dx.doi.org/10.1016/j.jallcom.2013.11.002

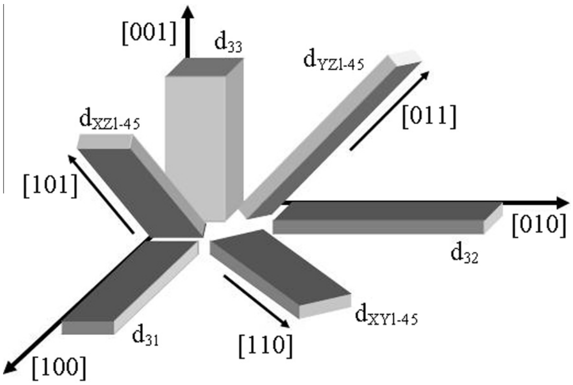

Fig. 1. Orientation of samples for studies of the piezoelectric tensor components.

$$(s_{jj})' = \left[\rho(2f_r l)^2\right]^{-1}, \tag{2}$$

$$|(d_{3j})'| = (k_{3j})'\sqrt{(s_{jj})'(\varepsilon_{33})'\varepsilon_0}, \tag{3}$$

$j = 1\ldots6$ is the index of elastic deformation in the matrix notation;

- for the longitudinal piezoelectric phenomenon for normal vibration along the length of a bar:

$$k_{33}^2 = \frac{\pi}{2}\frac{f_r}{f_a}\tan\left(\frac{\pi}{2}\frac{f_a - f_r}{f_r}\right), \tag{4}$$

$$s_{33} = \left[\rho(2f_r l)^2(1 - k_{33}^2)\right]^{-1}, \tag{5}$$

$$|d_{33}| = k_{33}\sqrt{s_{33}\varepsilon_{33}\varepsilon_0} \tag{6}$$

where f_r and f_a are frequencies of the series and parallel resonances and $\rho = 1801\ \mathrm{kg\ m^{-3}}$ [4].

The damping coefficient was given as the inverse amplitude of the signal of resonance vibrations. The signs of the piezoelectric tensor components were determined by the static method, measuring changes in the electric charge on the surfaces of the cubic sample appearing under uniaxial compressing stress.

The pyroelectric coefficient was determined by the quasi-stationary method on the basis of changes in the electric charge generated by temperature changes on the surface of a thin plate cut out in perpendicular to the twofold axis. Changes in the charge were measured by an electrometer to the accuracy of 10^{-14} C. The complex dielectric permittivity was investigated at low frequencies ranging from 500 Hz up to 1 MHz by a meter HP4284A at the intensity of the measuring field of 1 V mm^{-1}. Piezoelectric and dielectric measurements were investigated in the range 100–300 K and pyroelectric measurements in the range 80–360 K, on heating and on cooling. The temperature was measured by chromel–FeAu thermocouple.

3. Results

3.1. Pyroelectric coefficient

At room temperature (295 K) the total pyroelectric coefficient takes the value $|p^\sigma| = 3.9\ \mu\mathrm{C\ m^{-2}\ K^{-1}}$ – the quasi-stationary method does not permit determination of the sign of the pyroelectric coefficient. In classical pyroelectric crystals of tourmaline $p^\sigma = 2.5\text{–}4.9\ \mu\mathrm{C\ m^{-2}\ K^{-1}}$, depending on the chemical composition [7]. Pyroelectric properties of only a few non-ferroelectric semiorganic crystals containing amine acids have been determined, the relevant data are given in the table below (Table 1).

Temperature changes in pyroelectric coefficient measured in the range 80–360 K are presented in Fig. 2. According to the thermodynamic analysis of Boguslawski [13] and Eckermann [14], the pyroelectric coefficient in higher temperatures can be described by a square function. For the crystals of Gly_3–$ZnCl_2$ this square function takes the form:

$$|p^\sigma| = 8.3 - 8.0\times10^{-3}T - 2.4\times10^{-5}T^2. \tag{7}$$

Table 1
Pyroelectric coefficients of non-ferroelectric semiorganic crystals at ambient temperature.

Crystal	p^σ ($\mu\mathrm{C\ m^{-2}\ K^{-1}}$)	Ref.
L-arginine – $HCl{\cdot}H_2O$	0.66	[8]
L-arginine – $HBr{\cdot}H_2O$	0.92	[8]
L-arginine – $HClO_3$	$\leq$0.04	[9]
L-arginine – $HBrO_3$	6	[9]
L-arginine – $H_3PO_4{\cdot}H_2O$	0.5	[10]
Glycine – L-alanine – HBr	16	[11]
γ-Glycine	13	[12]

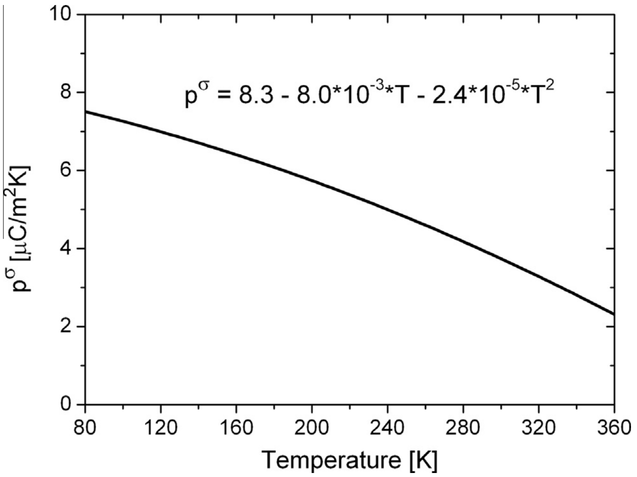

Fig. 2. Temperature dependence of pyroelectric coefficient of Gly_3–$ZnCl_2$ crystals.

Unfortunately, the lack of literature data on temperature expansion of Gly_3–$ZnCl_2$ crystals does not permit calculation of the true pyroelectric coefficient p^η.

3.2. Piezoelectric and elastic properties

Table 2 presents the components of piezoelectric tensor of Gly_3–$ZnCl_2$ crystal and for the sake of comparison the corresponding values obtained for a few non-ferroelectric crystals containing amine acids at room temperature. The components of the tensor of elastic susceptibility and their temperature derivatives measured at 295 K are given in Table 3.

Temperature changes in the elastic susceptibility, attenuation of resonance vibrations and piezoelectric coefficient are illustrated in Figs. 3–5.

Elastic susceptibility measured along the main crystallographic directions in the range 100–300 K does not show any anomalies and is almost linearly temperature dependent. In the directions [100] and [010] the attenuation of resonance vibrations reach a maxima at 220 K increase by 30–35%. At the same temperature the components d_{31} and d_{32} reach a small maxima increase by about $0.1\times10^{-12}\ \mathrm{m\ V^{-1}}$. The most pronounced is the direction [001], for which the piezoelectric effect at 220 K increases by 45%, while the attenuation shows a twofold increase.

Temperature changes in the resonance vibrations in three samples (labelled in Fig. 1 as $d_{XYl\text{-}45^\circ}$, $d_{XZl\text{-}45^\circ}$, $d_{YZl\text{-}45^\circ}$) cut out at the inclination of 45° with respect to the main crystallographic axes were also determined. In these samples at 220 K small anomalies in attenuation were observed, while in the piezoelectric coefficient only the temperature slope was changed. Making use of the transformation relations of the tensors, Figs. 6 and 7 present the temperature dependencies of shear components of the piezoelectric tensor and the tensor of elastic susceptibility.